

# Modeling of Lithium Battery Cells for Plug-In Hybrid Vehicles

Dong-Hyun Shin<sup>\*</sup>, Jin-Beom Jeong<sup>\*</sup>, Tae-Hoon Kim<sup>\*</sup>, and Hee-Jun Kim<sup>†</sup>

<sup>\*</sup>Electronic System R&D Center, Korea Automotive Technology Institute, Chungnam, Korea

<sup>†</sup>School of Electrical Engineering and Computer Science, Hanyang University, Seoul, Korea

## Abstract

Online simulations are utilized to reduce time and cost in the development and performance optimization of plug-in hybrid electric vehicle (PHEV) and electric vehicles (EV) systems. One of the most important factors in an online simulation is the accuracy of the model. In particular, a model of a battery should accurately reflect the properties of an actual battery. However, precise dynamic modeling of high-capacity battery systems, which significantly affects the performance of a PHEV, is difficult because of its nonlinear electrochemical characteristics. In this study, a dynamic model of a high-capacity battery cell for a PHEV is developed through the extraction of the equivalent impedance parameters using electrochemical impedance spectroscopy (EIS). Based on the extracted parameters, a battery cell model is implemented using MATLAB/Simulink, and charging/discharging profiles are executed for comparative verification. Based on the obtained results, the model is optimized for a high-capacity battery cell for a PHEV. The simulation results show good agreement with the experimental results, thereby validating the developed model and verifying its accuracy.

**Key words:** Battery Equivalent Circuit, Constant Phase Element (CPE), Dynamic Simulation, Electrochemical Impedance Spectroscopy (EIS), PHEV, Lithium Battery

## I. INTRODUCTION

On account of rising oil prices and the need to reduce the amount of greenhouse gases meet the recommendations of the UN Framework Convention on Climate Change, there has been active research on environmentally friendly, high-efficiency vehicles, including hybrid electric vehicles (HEVs), plug-in hybrid electric vehicles (PHEVs), and electric vehicles (EVs). As the specifications required for the parts used in these environmentally friendly vehicles are highly variable in the developmental phase, model-based simulations are performed to reduce the time and cost required for developing and optimizing the systems and their parts.

The performance of an environmentally friendly vehicle is significantly affected by its high-capacity battery system.

However, it is difficult to implement a simulation model of a battery system that accurately reflects the battery's dynamic characteristics during charging and discharging because of its nonlinear electrochemical properties. Accordingly, simulations are generally performed using a simplified battery model or a hardware-in-the-loop simulation (HILS) associated with the actual battery [1], [2]. Although research has been carried out on this type of battery modeling [3]-[5], most studies have dealt with low-capacity batteries in the range of several ampere-hours, and there have been very few attempts to validate these models with studies or experiments on high-capacity battery cells with the dozens of ampere-hours required for PHEVs or EVs.

This study examined various equivalent impedance models for the 20Ah lithium battery cells of PHEVs and elicited parameters for each of their state of charge (SOC) using electrochemical impedance spectroscopy (EIS) to enable implementation of high-capacity battery cell models with MATLAB/Simulink. Furthermore, charging/discharging profiles were selected to compare dynamic characteristics between the elicited models and actual battery cells. The simulation results were also compared against actual

Manuscript received May 11, 2012; revised Mar. 6, 2013

Recommended for publication by Associate Editor John Shen.

<sup>†</sup>Corresponding Author: [hjkim@hanyang.ac.kr](mailto:hjkim@hanyang.ac.kr)

Tel: +82-31-400-5164, Fax: +81-836-85-9401, Hanyang University

<sup>\*</sup>Electronic System R&D Center, Korea Automotive Technology Institute, Korea

<sup>†</sup>School of Electrical Engineering and Computer Science, Hanyang University, Korea

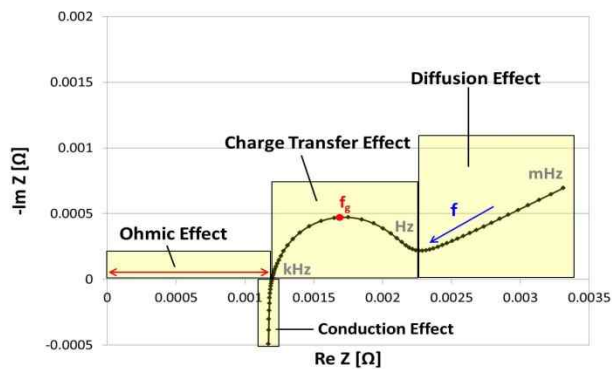


Fig. 1. Nyquist plot of electrochemical reaction.

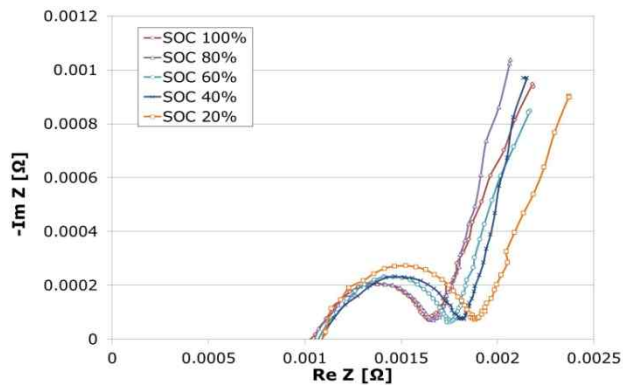



Fig. 2. Impedance spectra for each SOC of a PHEV lithium battery.

TABLE I  
SPECIFICATIONS OF PHEV BATTERY CELL

	Type	Lithium Polymer
	Rated Capacity	20 [Ah]
	Rated Voltage	3.6 [V]
	Maximum Voltage	4.2 [V]
	Minimum Voltage	3.0 [V]

experimental results according to the selected profiles to calculate the error rate of each model. Based on the calculated error rates, the accuracy of each model was analyzed and the most appropriate model was selected for high-capacity battery cells for PHEVs.

## II. LITHIUM BATTERY CHARACTERISTICS AND ELECTROCHEMICAL IMPEDANCE SPECTROSCOPY

A battery is an electrochemical device that converts chemical energy into electric energy during discharging and does the opposite during charging. Therefore, the electrochemical properties of a battery determine its dynamic and static characteristics, and accurately analyzing and representing these properties enables the implementation of a

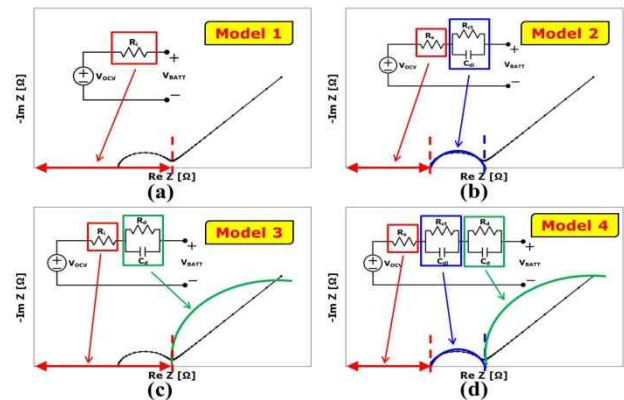


Fig. 3. Estimation method of the equivalent impedance for each model. [SOC 80%,  $R_s = 1.13\text{m}\Omega$ ,  $R_{ct} = 0.42\text{m}\Omega$ ,  $C_{dl} = 8.8\text{F}$ ,  $R_d = 1.88\text{m}\Omega$ ,  $C_d = 13375\text{F}$ ].

model that closely represents the characteristics of an actual battery.

The major internal electrochemical reactions of a lithium battery include the Ohmic loss, the charge transfer loss related to the properties of the interface between the electrode and the electrolyte, and the diffusion loss [6]. The Ohmic loss is shown as the value at the intersection with the real axis in the impedance spectrum; the charge transfer effect is exhibited as a large semicircle in the high-frequency region; and the diffusion effect, which is exhibited in the low-frequency region, yields a straight line with a specific slope or sometimes a large semicircle depending on the type of battery. Fig. 1 shows a Nyquist plot of the electrochemical reaction of a lithium battery.

EIS refers to a technique which involves applying a small perturbation to each frequency range of the impedance to be measured, analyzing the current (or voltage) in the response to the applied small perturbation, and eliciting the parameters of the impedance model consisting of resistors, capacitors, and inductors. The impedance models that can be constructed with EIS vary depending on how the elements that represent each electrochemical property are configured [7].

In this study, a WEIS500 electrochemical workstation was used to acquire the battery impedance spectrum and to measure the impedance in the 10mHz to 1kHz frequency range. In order to guarantee linearity in the experiment, the perturbation current was restricted to 5% or less of the charge, and it was ensured that there was no variation in the amount of electric charge before or after the experiment. The impedance was measured in 20% intervals from 20% to 100% of the SOC at room temperature (25°C). Table 1 outlines the specifications of the PHEV high-capacity lithium battery cell used in this study, and Fig. 2 shows the impedance spectrum of the cell measured for each SOC.

Four equivalent impedance models were constructed to model the corresponding cell, as shown in Fig. 3, and the parameters were extracted by fitting a curve for each model

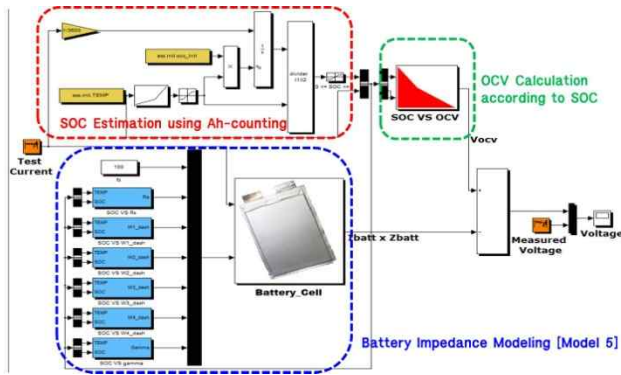


Fig. 4. MATLAB/Simulink block diagram.

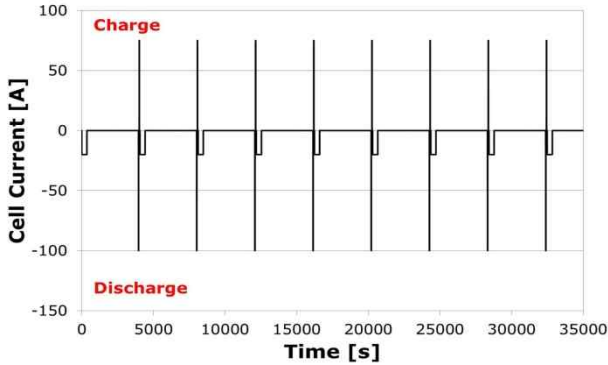


Fig. 5. Current waveform of the HPPC profile.

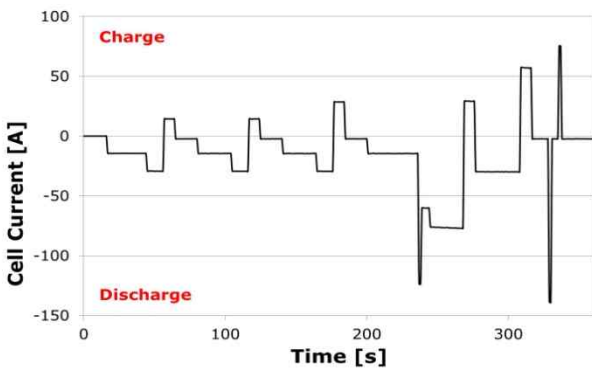


Fig. 6. Current waveform of the CDCL profile.

based on the measured impedance spectrum. The accuracy of the fitting was measured using the chi-square test. If the measured value converges within 1%~2%, this means that the measurement data and the equivalent circuit model are closely correlated. Fig. 3(a) depicts an equivalent model (Model 1) consisting of a simple resistor, defined as the internal resistance  $R_i$ , which is the sum of the series resistance  $R_s$  and the charge transfer resistance  $R_{ct}$ . Fig. 3(b) is a model that reflects the resistance region and the charge transfer region (Model 2). It is an equivalent parallel RC circuit of the high-frequency charge transfer region and the series resistance  $R_s$ . Fig. 3(c) is a model that reflects the resistance region and the diffusion region (Model 3). It is an equivalent parallel RC circuit of the low-frequency diffusion region and the internal resistance  $R_i$ . Finally, Fig. 3(d) is a model that incorporates all of the regions (Model 4) consisting of the series resistance  $R_s$  and two parallel

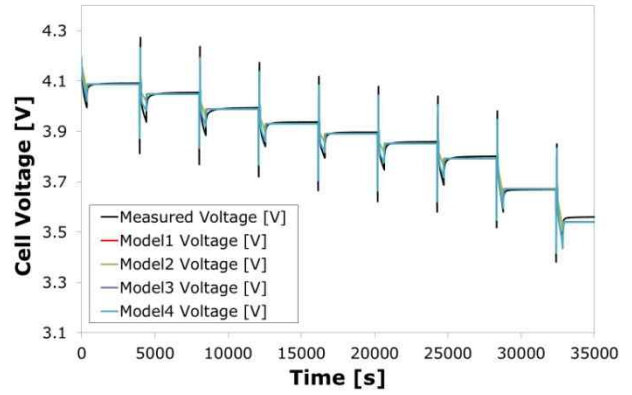


Fig. 7. Simulation results of the HPPC pattern for each model.

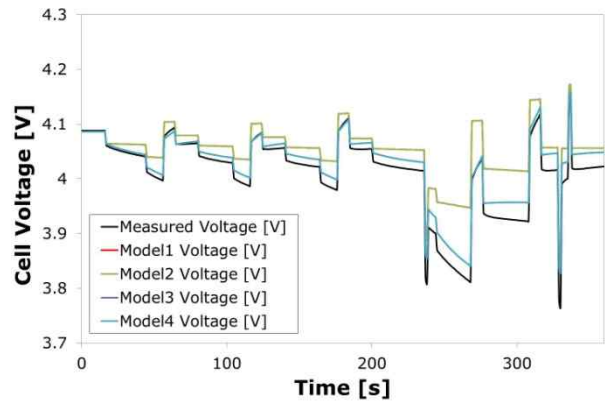


Fig. 8. Simulation results of the CDCL pattern for each model.

RC circuits.

### III. SIMULATION AND VALIDATION RESULTS

#### A. Simulation Using MATLAB/Simulink

For the simulation of the elicited lithium battery cell model, a dynamic characteristics model was created based on the equivalent impedance and the implemented battery model using MATLAB/Simulink, as shown in Fig. 4. Applying the conventional ampere-hour counting method and a compensation method that utilizes the open-circuit voltage (OCV) to estimate the SOC, the implemented battery cell model calculates the terminal voltage of the battery cell by reflecting the OCV according to the estimated SOC and the voltage variation in the dynamic characteristics model. The impedance parameters of the dynamic characteristics model are modified and applied to the model in real time through a look-up table (LUT), and  $V_{batt}$ , the battery cell's terminal voltage, can be calculated using (1).

$$V_{batt} = V_{OCV} + (I_{batt} \times Z_{batt}) \quad (1)$$

#### B. Validation and Consideration of Each Model

In order to compare the properties of the simulation model obtained in this study and those of an actual battery cell,

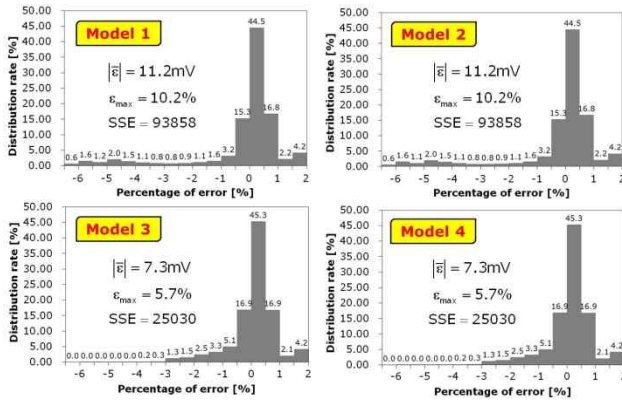


Fig. 9. Error rate comparison of the HPPC pattern for each model.

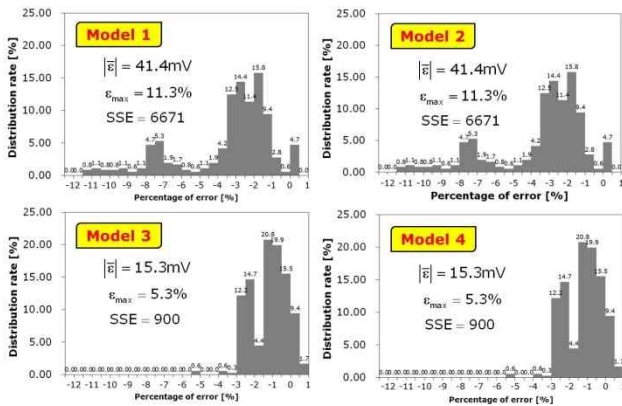


Fig. 10. Error rate comparison of the CDCL pattern for each model.

charging and discharging experiments were conducted according to the profiles shown in Figs. 5 and 6, which are explained in the PHEV Battery Test Manual issued by the Idaho National Laboratory (INL) of the U.S. Department of Energy [8]. The hybrid pulse power characterization (HPPC) test profile shown in Fig. 5 is effective for comparing the steady-state characteristics of each SOC of the model and the actual battery, because charging and discharging pulses are applied while the SOC is discharged to 10%. The charging-depleting cycle life (CDCL) shown in Fig. 6 is adequate for comparing the dynamic characteristics of the simulation model and the actual battery, because the charging and discharging are repeated frequently.

In order to compare the accuracies of the equivalent models by analyzing the results of the simulations and experiments, the difference between the measured voltage and the simulation voltage was divided by the operating voltage range from 0% to 100% of the battery cell's SOC to calculate the error rate ( $\epsilon$ ), as shown in (2). The error rate quantitatively indicates how accurately the model used in the simulation reflects the properties of an actual battery. The smaller the error rate, the better the model represents an actual battery. In addition, the average value of the absolute error ( $|\epsilon|$ ), the maximum error rate ( $\epsilon_{max}$ ), and the sum of the squared errors (SSE) were

calculated to compare the accuracies of the models. Fig. 7 and 8 display the simulation results of each model according to the HPPC and CDCL test patterns, and Figs. 9 and 10 show the error rates calculated for each model.

Error Rate[%]

$$= \frac{(Measured\ voltage) - (Simulation\ voltage)}{(Operating\ voltage\ range)} \times 100 \quad (2)$$

Based on the validation results of each elicited model, it was confirmed that there is no difference in terms of the simulation voltage waveform and error distribution rate between Models 2 and 4, which included the impedance of the high-frequency charge transfer region, and Models 1 and 3, which did not include a high-frequency region. This suggests that in the HPPC and CDCL testing of the high-capacity battery cell used in this study, the influence from the equivalent impedance of the charge transfer region was minimal, resulting in almost no difference in the waveform and error rate calculation. Furthermore, it was confirmed that Models 3 and 4 provide a closer representation of the actual voltage and have smaller average values of the absolute error and maximum error rates than Models 1 and 2. Accordingly, it can be concluded that including the equivalent impedance, which indicates the diffusion region (rather than the charge transfer region), provides a more accurate model of the PHEV high-capacity battery cell used in this study.

### C. Complementing the Model Using CPE (Model 5)

As explained in the previous section, the charge transfer region has an insignificant influence on the battery's dynamic characteristics, whereas the diffusion region has the predominant influence. Therefore, it is expected that modeling the low-frequency diffusion region more accurately will enhance the accuracy of the battery model. As the time constant from diffusion typically ranges from several seconds to a few minutes, the properties of this region are dominant in the low frequency range (below 1Hz) of the impedance spectrum.

As shown in Fig. 1, the diffusion region in the impedance spectrum is in a linear form where the real and imaginary components increase proportionally. There are limitations in representing it with a single parallel RC circuit that forms a semicircle between the real and imaginary impedance components. Circuit elements used to accurately represent diffusion include the Warburg element and the constant phase element (CPE) [9-11]. The Warburg element demonstrates the typical diffusion pattern of a battery that uses plate electrodes and models semi-infinite diffusion. The Warburg element is a straight line with a slope of  $-45^\circ$  in the impedance spectrum, as shown in Fig. 11, and it can be mathematically expressed as (3).



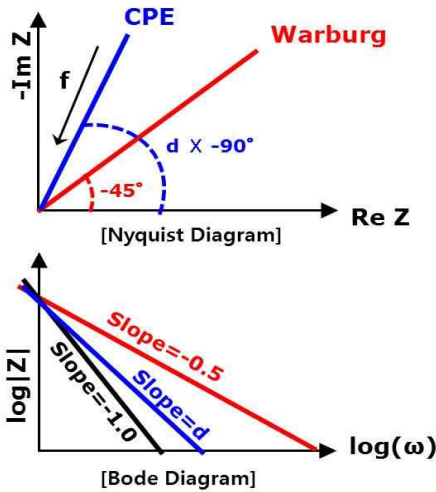


Fig. 11. Comparison of the characteristics of the Warburg element and the CPE.

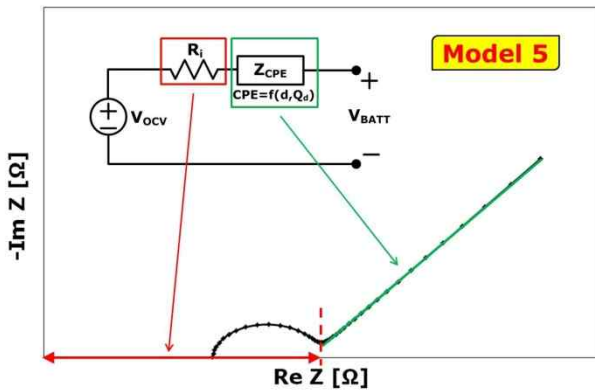


Fig. 12. Estimation method of the equivalent impedance for model 5.

$$Z_{warburg}(s) = Q / s^{0.5} \tag{3}$$

However, according to the EIS result of the PHEV battery cell used in this study, the impedance spectrum has a slope greater than  $-45^\circ$  (Fig. 2) in the diffusion region, which poses limitations on modeling the diffusion region with the Warburg element. On the other hand, as shown in Fig. 11, the frequency across the CPE decreases because of the effect from variable  $d$ , which increases the imaginary component of the impedance, allowing the CPE to have a greater slope and rendering it useful for representing the battery cell's diffusion region. Therefore, model 5 was formed by using the CPE as in Fig. 12. Since it is mainly used to model the electrical double-layer effect, the CPE simulates an imperfect capacitor and has a specific slope in the frequency domain according to the value of  $d$  [9,12]. The CPE can be described by (4), where  $Q$  is the pseudo-capacitance and  $d$  is a variable with a value between 0 and 1. If  $d = 1$ , the CPE is equivalent to a pure capacitor; if  $d = 0.5$ , the CPE shows impedance characteristics identical to those of the Warburg element; and if  $d = 0$ , the CPE is equivalent to a resistor. Unlike a parallel RC circuit, the CPE is not a

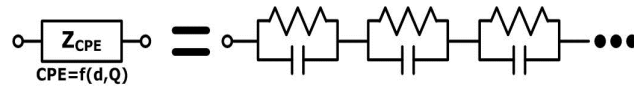


Fig. 13. CPE impedance approximation model.

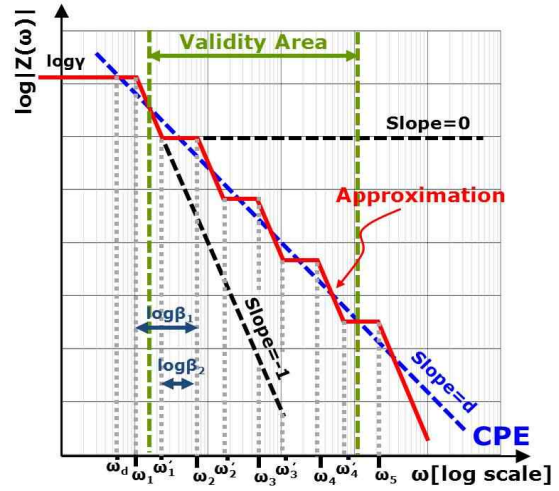


Fig. 14. Technique for simplifying CPE impedance using Bode plot.

function of an integer degree in the frequency domain and it cannot have an integer value, except for the cases where  $d = 0$  or 1. Since it is difficult to express a function that is not of an integer degree in the frequency domain with MATLAB/Simulink, it is not feasible to apply (4) in its intrinsic form to implement the simulation model. Accordingly, the CPE must be converted from the frequency domain to the time domain, as shown in (5). However, a simulation model employing (5) must undergo convolution in order to transform the voltage response in the frequency domain to the time domain. However, this is not practical due to mathematical complexity [13].

$$Z_{CPE}(s) = Q / s^d \tag{4}$$

$$Z_{CPE}(t) = Q \times t^{d-1} / \Gamma(d) \tag{5}$$

The CPE parameters were extracted from the impedance spectrum measured with the EIS per the estimated SOC and then approximated as five parallel RC circuits (Fig. 13) to implement a MATLAB/Simulink model capable of real-time simulations [12]. The fundamental hypothesis that allows the approximation of the CPE as five parallel RC circuits is established from the concept that two models with an equal impedance component at a specific frequency have the same properties. In order to express the CPE of (4) on a Bode plot, which depicts frequency response characteristics, the log function was used to obtain the gain, as in (6). The gain is plotted as a monotone function with a slope of  $d$  on the Bode plot, as indicated by the blue dotted line in Fig. 14. The gain properties of the CPE can be approximated as the gain of five

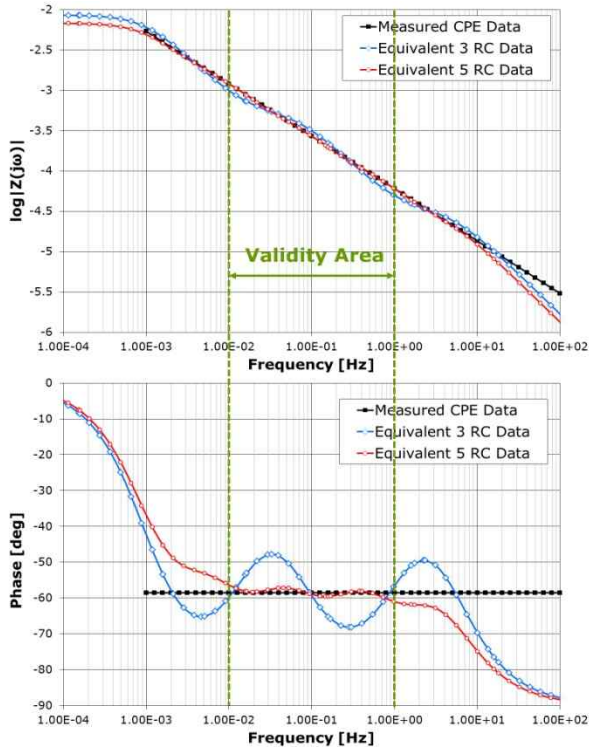


Fig. 15. Bode plot of CPE impedance and the linearization model of parallel RC ladder. [SOC 80%,  $d = -0.61$ ,  $R_s = 1.13\text{m}\Omega$ ,  $\omega_1 = 0.00628\text{ rad/s}$ ,  $\omega_5 = 62.8\text{ rad/s}$ ,  $\beta_1 = 10$ ,  $\beta_2 = 2.455$ ,  $\gamma = 0.0044$ ].

parallel RC circuits with a slope of -1, indicated by the red line in Fig. 14, and the approximated parallel RC circuits can be described by (7) with four zeroes and five poles.

$$G = \log |Z_{CPE}(j\omega)| = \log Q - d \times \log(\omega) \quad (6)$$

$$\begin{aligned} Z_{CPE}(s) &\approx Z_{CPE, App}(s) \\ &= \gamma \times \frac{1+s/\omega'_1}{1+s/\omega_1} \times \frac{1+s/\omega'_2}{1+s/\omega_2} \times \dots \times \frac{1}{1+s/\omega_5} \end{aligned} \quad (7)$$

On the Bode plot, the distance between  $\omega_{k+1}$  and  $\omega_k$  as well as the distance between  $\omega_{k+1}$  and  $\omega'_k$  of (7) can be defined by using  $\beta_1$  and  $\beta_2$  of (8) and (9).

$$\log \beta_1 = \log \omega_{k+1} - \log \omega_k \quad (8)$$

$$\log \beta_2 = \log \omega_{k+1} - \log \omega'_k \quad (9)$$

In addition, as the CPE was approximated as multiple parallel RC circuits with slopes of both 0 and -1, the following relationships can be established between the zeros ( $\omega'_k$ ) and the poles ( $\omega_k$ ).

- The slope between  $\omega'_k$  and  $\omega_{k+1} = 0$

$$\frac{\log |Z(\omega'_{k+1})| - \log |Z(\omega'_k)|}{\log \beta_2} = 0 \quad (10)$$

- The slope between  $\omega_k$  and  $\omega'_k = -1$

$$\frac{\log |Z(\omega'_k)| - \log |Z(\omega_k)|}{\log \beta_1 - \log \beta_2} = -1 \quad (11)$$

- The slope between  $\omega_k$  and  $\omega_{k+1} = d$

$$\frac{\log |Z(\omega_{k+1})| - \log |Z(\omega_k)|}{\log \beta_1} = d \quad (12)$$

Rearranging (8)-(12),  $\beta_1$  and  $\beta_2$  can be calculated with (13) and (14).

$$\beta_1 = \sqrt[k]{\omega_{k+1} / \omega_1} \quad (13)$$

$$\beta_2 = 10^{(1+d) \times \log \beta_1} \quad (14)$$

For the approximation of the CPE impedance to the RC parallel circuit, the CPE parameter  $d$  was extracted after measurement of the battery's impedance with EIS. As a result, three variables ( $\gamma$ ,  $\omega_1$ , and  $\omega_5$ ) were determined. However, this equivalence method is only valid in a specific frequency range; the minimum frequency was set as  $\omega_{\min}$ , and the maximum frequency was set as  $\omega_{\max}$  (the green dotted line in Fig. 13). In the present study, in consideration of the impedance characteristics of the analyzed battery,  $\omega_{\min}$  was set to 1mHz, and  $\omega_{\max}$  was set to at 5kHz. In addition,  $\omega_1$  was set to 1/10 of the frequency of  $\omega_{\min}$  ( $\omega_1 = 0.1\omega_{\min}$ ), and  $\omega_5$  was set to 10 times  $\omega_{\max}$  ( $\omega_5 = 10\omega_{\max}$ ). The low frequency gain  $\gamma$  is expressed in (16).

$$\log \omega_d = \log \omega_1 - \log \beta_2 / 2 \quad (15)$$

$$\gamma \approx |Z_{CPE}(\omega_d)| \quad (16)$$

Fig. 15 shows the battery's CPE components obtained with EIS when the SOC of the battery was at 80%, and the results of simplifying the CPE components as three and five parallel RC circuits. With three parallel RC circuits, the phase and magnitude varied significantly from the CPE components, posing serious limitations for use as equivalent circuits. However, using five parallel RC circuits produced results almost identical to those of the CPE components, indicating that the CPE properties of the low-frequency region were adequately implemented.

#### D. Validation of the Complemented Model

In order to validate the accuracy of the complemented model, the experimental results and the simulation results were compared according to the HPPC profile (Fig. 16) and the CDCL profile (Fig. 17) using the same procedure as the previous validation process. As indicated by Figs. 16 and 17, Model 5, which employed the CPE impedance, modeled the properties of the actual battery cell more accurately than Models 1-4, confirming the need for accurate modeling of the diffusion region and the validity of the approximation of the

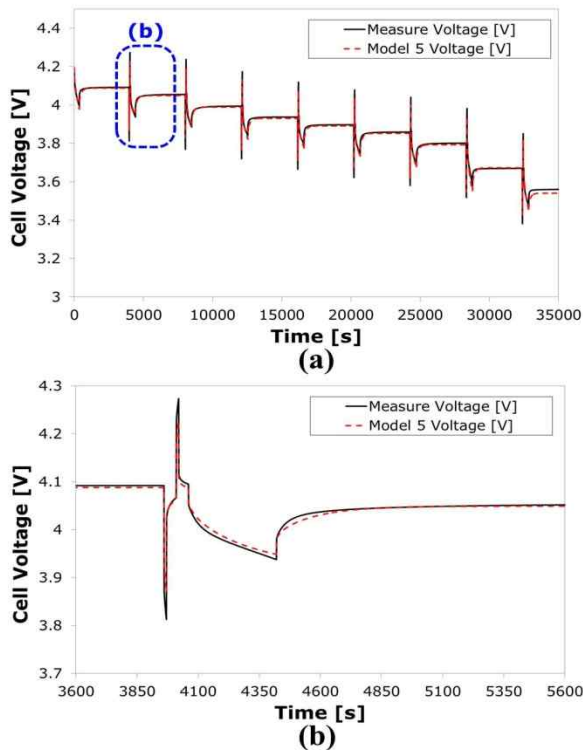


Fig. 16. HPPC pattern simulation results of Model 5. (a) Comparison of voltages of Model 5. (b) Comparison of specific voltages of Model 5.

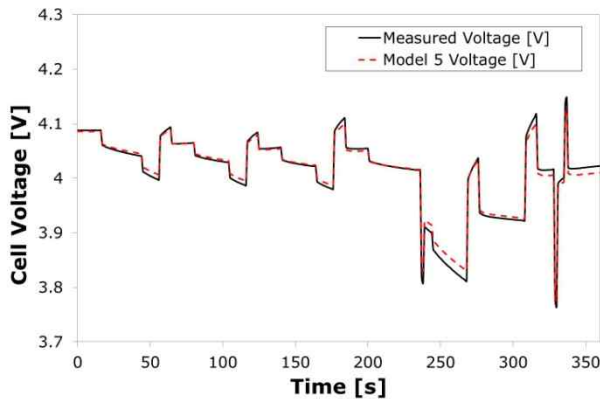


Fig. 17. CDCL profile simulation results of Model 5.

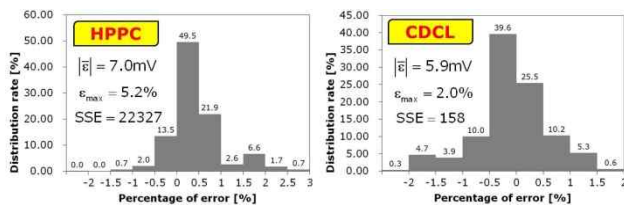


Fig. 18. Model 5's error rate for each profile.

CPE impedance using a Bode plot. In terms of error rate, the maximum error rates in the HPPC and CDCL profiles were 5.2% and 2.0%, respectively, and the error rates mostly ranged between -1% and 1%. Compared with Models 3 and 4, Model 5's error rate distribution was within a smaller error rate range,

and the CDCL experiment showed more than twice an improvement in accuracy. However, since the HPPC is a profile with prominent steady-state characteristics, using a model that employs the CPE improved the accuracy only slightly.

#### IV. CONCLUSIONS

In this study, high-capacity lithium battery cell modeling was carried out for a real-time simulation in order to reduce the time and cost required to optimize and develop environmentally friendly vehicle systems. Various equivalent impedance models were examined for high-capacity 20 Ah lithium battery cells for PHEVs, the parameters for each SOC of the cells were extracted using EIS, the implementation of a high-capacity battery cell model was enabled with MATLAB/Simulink. Furthermore, charging and discharging profiles were selected for a comparison of the dynamic properties between the estimated models and the actual battery cell. The experimental results according to the selected profiles were compared with the simulation results of each model to calculate the error rate. Based on the calculated error rates, the accuracies of the models were compared and the most appropriate modeling technique was selected for implementing a model of a high-capacity battery cell for PHEVs. The simulation results were very similar to the experimental results, and the proposed modeling and simulation methods are expected to be instrumental for modeling the battery pack systems of PHEVs.

#### ACKNOWLEDGMENT

The research was supported by the International Science and Business Belt Program through the Ministry of Education, Science and Technology (2012K001568).

#### REFERENCES

- [1] S. Nabi, M. Balike, J. Allen, and K. Rzemien, "An overview of hardware-in-the-loop testing systems at Visteon," *SAE paper*, 2004-01-1240, Jan. 2004.
- [2] A. Dhaliwal, S. C. Nagaraj, and S. Ali, "Hardware-in-the-loop simulation for hybrid electric vehicles-an overview, lessons learnt and solutions implemented," *SAE paper*, 2009-01-0735, Apr. 2009.
- [3] T. K. Dong, A. Kirchev, F. Mattera, J. Kowal, and Y. Bultel, "Dynamic modeling of Li-ion batteries using an equivalent electrical circuit," *J. Electrochem. Soc.*, Vol. 158, No. 3, pp. A326-A336, Jan. 2011.
- [4] H. Zhang and M.-Y. Chow, "Comprehensive dynamic battery modeling for PHEV applications," in *Proc. IEEE Power and Energy Society General Meeting*, Jul. 2010.
- [5] Y. Guezennec, W. Choi, and T. Choi, "Optimized dynamic battery model suited for power based vehicle energy simulation," *International Journal of Automotive Technology*, Vol. 13, No. 1, pp. 133-141, Jul. 2012.
- [6] Andreas Jossen, "Fundamentals of battery dynamics," *J. Power Sources*, Vol. 154, pp. 530-538, Dec. 2006.

- [7] J.-H. Lee and W. Choi, "Novel state-of-charge estimation method for lithium polymer batteries using electrochemical impedance spectroscopy," *Journal of Power Electronics*, Vol. 11, No. 2, pp. 237-243, Feb. 2011.
- [8] Idaho National Lab., Battery test manual for plug-in hybrid electric vehicles, Rev. 0, Mar. 2008.
- [9] S.-H. Kim, W. Choi, K.-B. Lee, and S. Choi, "Advanced dynamic simulation of supercapacitors considering parameter variation and self-discharge," *IEEE Trans. Power Electron.*, Vol. 26, No. 11, pp. 3377-3385, Nov. 2011.
- [10] S. Buller, M. Thele, R. W. A. A. D. Doncker, and E. Karden, "Impedance-based simulation models of supercapacitors and Li-ion batteries for power electronic applications," *IEEE Trans. Ind. Appl.*, Vol. 41, No. 3, pp. 742-747, May/Jun. 2005.
- [11] J. Bisquert, G. Garcia-Belmonte, P. Bueno, E. Longo, and L.O.S. Bulhões, "Impedance of constant phase element (CPE)-blocked diffusion in film electrodes," *J. Electroanal. Chem.*, Vol. 452, pp. 229-234, Mar. 1998.
- [12] M. Montaru, and S. Pelissier, "Frequency and temporal identification of a Li-ion polymer battery model using fractional impedance," *Oil Gas Science and Technology*, Vol. 65, No. 1, pp. 67-78, Jan./Feb. 2010.
- [13] P. J. Mahon, G. L. Paul, S. M. Keshishian, and A. M. Vassallo, "Measurement and modelling of the high-power performance of carbon-based supercapacitors," *J. Power Sources*, Vol. 91, pp. 68-76, Mar. 2000.



**Dong-Hyun Shin** received his B.S. in Mechanical Engineering from Sungkyunkwan University, Seoul, Korea, in 1999, his M.S. in Mechatronics Engineering from the Gwangju Institute of Science and Technology (GIST), Gwangju, Korea, in 2001, and his Ph.D. in the Department of Mechatronics Engineering from Hanyang

University, Seoul, Korea, in 2012. His current research interests include the design of hybrid electric vehicles and the optimal control and modeling of energy storage systems. He is currently a Senior Researcher at the Electronic System R&D Center, Korea Automotive Technology Institute (KATECH), Chungnam, Korea.



**Jin-Beom Jeong** received his B.S. and M.S. in Electrical Engineering from Hanyang University, Ansan, Korea, in 2001 and 2003, respectively, and his Ph.D. from the Department of Electronic, Electrical, Control and Instrumentation Engineering, Hanyang University, in 2007. Since 2007, he has been with the Electronic System R&D Center,

Korea Automotive Technology Institute (KATECH), Chungnam, Korea, where he is currently a Senior Researcher. His current research interests include switching power converters, power electronic systems, BMS, battery systems, and EV/PHEV charging systems.



**Tae-Hoon Kim** received his B.S. and M.S. in Electrical Engineering from Soongsil University, Seoul, Korea, in 2009 and 2011, respectively. His current research interests include power electronic systems, BMS, battery systems, and HILS for PHEV/EVs. He is currently a Researcher at the Electronic System R&D Center, Korea Automotive

Technology Institute (KATECH), Chungnam, Korea.



**Hee-Jun Kim** received his B.S and M.S. in Electronics Engineering from Hanyang University, Seoul, Korea, in 1976 and 1978, respectively, and his Ph.D. in Electronics Engineering from Kyushu University, Kyushu, Japan, in 1986. Since 1987, he has been with the Department of Electronic Systems Engineering, Hanyang University,

Ansan, Korea, where he is currently a Professor. His current research interests include switching power converters, electronic ballasts, soft switching techniques, and analog signal processing. Dr. Kim is a senior member of IEEE.